

1 A metabolic CRISPR-Cas9 screen in Chinese hamster ovary 2 cells identifies glutamine-sensitive genes

3
4 Karen Julie la Cour Karottki¹, Hooman Hefzi^{2,4,5}, Songyuan Li¹, Lasse Ebdrup Pedersen¹,
5 Philipp Spahn^{2,4}, Chintan Joshi^{2,4}, David Ruckerbauer^{6,7}, Juan Hernandez Bort⁶, Alex
6 Thomas², Jae Seong Lee⁸, Nicole Borth^{6,7}, Gyun Min Lee³, Helene Fastrup Kildegaard^{1,*},
7 Nathan E. Lewis^{2,4,5,*}

8
9 ⁽¹⁾The Novo Nordisk Foundation Center For Biosustainability, Technical University Of Denmark, Denmark
10 ⁽²⁾The Novo Nordisk Foundation Center For Biosustainability At The University Of California, San Diego, USA

11 ⁽³⁾Department Of Biological Sciences, Kaist, 291 Daehak-Ro, Yuseong-Gu, Daejeon 305-701, Republic Of Korea

12 ⁽⁴⁾Department of Pediatrics, University of California, San Diego, USA

13 ⁽⁵⁾Department of Bioengineering, University of California, San Diego, USA

14 ⁽⁶⁾Austrian Centre of Industrial Biotechnology, Vienna, Austria

15 ⁽⁷⁾University of Natural Resources and Life Sciences, Vienna, Austria

16 ⁽⁸⁾Department of Molecular Science and Technology, Ajou University, Suwon 16499, Republic of Korea

17 *Equal contribution, Correspondence to: Nathan E. Lewis, nlewisres@ucsd.edu

18

19

20 **Keywords:** CHO, CRISPR pooled screen, glutamine, metabolism¹

¹ **Abbreviations:** α kgdhc - alpha ketoglutarate dehydrogenase complex; Cas9 – CRISPR-associated protein 9; CHO – Chinese hamster ovary; CPM - counts per million; CRISPR – clustered regularly interspaced short palindromic repeats; DAPI – 4',6-diamidino-2-phenylindole; GFP – green fluorescent protein; GLS - glutaminase; GLUL - glutamine synthetase; gRNA – guide RNA; Mgat1 - mannosyl (alpha-1,3)- glycoprotein beta-1,2-N-acetylglucosaminyltransferase; NGS – next generation sequencing ; RNAi – RNA interference; TALEN - transcription activator-like effector nucleases; VCD – viable cell density; ZFN – zinc-finger nuclease

21

22

Abstract

23 Over the past decades, optimization of media formulation and feeding strategies have fueled
24 a many-fold improvement in CHO-based biopharmaceutical production. While Design of
25 Experiments (DOE) and media screens have led to many advances, genome editing offers
26 another avenue for enhancing cell metabolism and bioproduction. However the complexity
27 of metabolism, involving thousands of genes, makes it unclear which engineering strategies
28 will result in desired traits. Here we developed a comprehensive pooled CRISPR screen for
29 CHO cell metabolism, including ~16,000 gRNAs against ~2500 metabolic enzymes and
30 regulators. We demonstrated the value of this screen by identifying a glutamine response
31 network in CHO cells. Glutamine is particularly important since it is often substantially over-
32 fed to drive increased TCA cycle flux but can lead to accumulation of toxic ammonia. Within
33 the glutamine-response network, the deletion of a novel and poorly characterized lipase,
34 *Abhd11*, was found to substantially increase growth in glutamine-free media by altering the
35 regulation of the TCA cycle. Thus, the screen provides an invaluable targeted platform to
36 comprehensively study genes involved in any metabolic trait.

37

38

39

40

41

42 Chinese hamster ovary (CHO) cells are the most commonly used mammalian cells for
43 biotherapeutic protein production and serve as the expression system of choice for the leading
44 biologics¹. Consequently, improving product quality and decreasing manufacturing costs in
45 CHO is of great interest to the biopharmaceutical industry. Since their first use in the late
46 1980s, final product titers from CHO cells have improved more than 50-fold, largely through
47 media and bioprocess optimization². Although effective, these empirical approaches are highly
48 variable, demand extensive labor, time, and resources, and may not translate directly to new
49 clones.

50 All biological processes that lead to protein production depend on metabolic building
51 blocks. Although CHO cell media are complex owing to their nutritional demands³ the two
52 main nutrients consumed are glucose and glutamine. These are often taken up in excess of the
53 cells growth needs⁴ leading to increased by-product formation of lactate and ammonia,
54 respectively, which are the two primary byproducts negatively affecting cell growth,
55 production and product quality⁵⁻⁸. The complexity and incomplete understanding of
56 metabolism, along with unique idiosyncrasies of individual CHO clones have stymied the
57 optimization of their metabolism. However, the release of CHO and Chinese hamster genome
58 sequences⁹⁻¹¹ and improved systems biology approaches^{3,12} have laid the groundwork for a
59 new era of targeted CHO cell line development, but the question of the best way to discover
60 and engineer targets remains open.

61 Several techniques can be used to knock out genes in CHO cells, such as zinc finger
62 nucleases (ZFNs)¹³, transcription activator-like effector nucleases (TALENs)¹⁴, and Clustered
63 Regularly Interspaced Short Palindromic Repeats (CRISPR). However, since the best genes to

64 knock out are often unclear, given >20,000 genes in the CHO genome, efficient, high-
65 throughput methods are needed to identify optimal genetic modifications. Although RNA
66 interference (RNAi) screening has been useful for identifying gene knockdowns¹⁵ providing a
67 desired trait in CHO cells¹⁶, the inability to achieve full knockout, a significant amount of off-
68 target effects¹⁷, and inconsistent results has limited their use¹⁸. On the other hand, CRISPR-
69 Cas9 can also be used for large-scale pooled screening while avoiding some of the pitfalls in
70 RNAi screens¹⁹. The method has been established in several cell lines and organisms, mainly
71 mouse and human, increasing the robustness for the next generation of forward genetic
72 screening methods¹⁹⁻²³.

73 With the intent of generating a platform for gaining insight into CHO cell metabolism,
74 we present a large-scale CHO-specific CRISPR-Cas9 knockout screen in CHO cells. We
75 generated a gRNA library targeting genes for enzymes and regulators involved in CHO cell
76 metabolism. We deployed CRISPR-Cas9 knockout screening against an industrially relevant
77 selection pressure, glutamine deprivation, and identified a network of genes regulating growth
78 in response to glutamine concentration. We highlight one gene for a novel and poorly
79 characterized lipase, *Abhd11*, which, upon deletion, we found to substantially increase growth
80 in glutamine-free media by altering the regulation of the TCA cycle.

81

82 **Results**

83 **Establishing a CRISPR knockout library in CHO cells**

84 We first generated CHO-S cell lines constitutively expressing Cas9 (CHO-S^{Cas9}) via
85 G418 selection followed by single cell sorting and expansion to obtain clonal populations for

86 subsequent gRNA library transduction. We validated the functionality of Cas9 in the clonal
87 cell lines by transfecting CHO-S^{Cas9} with a gRNA targeting *Mgat1* and quantifying the cleavage
88 efficiency by indel analysis of the target region (Supplementary Table S1). To generate the
89 CRISPR knockout library, we designed a large CHO-specific gRNA library containing 1-10
90 gRNAs/gene for genes encoding enzymes and regulators of CHO metabolism. Genes selected
91 for inclusion were obtained from the genome scale metabolic model of CHO³, metabolism-
92 associated GO terms, and transcription factors that regulate the aforementioned genes (based
93 on annotation from Ingenuity Pathway Analysis²⁴). The library consists of 15,654 gRNAs
94 against 2,599 genes (1,765 genes from the model, 782 from GO terms, and 52 transcription
95 factors)(Supplementary Datafile 1). gRNAs were synthesized by CustomArray Inc. and
96 subsequently packaged into lentiviruses. CHO-S^{Cas9} cells were then transduced with the gRNA
97 library at low multiplicity of infection (MOI) (Supplementary Methods and Results) to ensure
98 only a single gRNA integration event per cell, generating a CHO CRISPR knockout library
99 for use in pooled screening (overview in Figure 1).

100

101 **Glutamine screening**

102 Glutamine is key to cell function and thus an important media component for animal
103 cell culture media formulations²⁵. However, glutamine is often oversupplied, and its
104 catabolism produces ammonia, a toxic byproduct that negatively impacts cell growth,
105 production, and product quality^{5,26-28}. Understandably, it is of interest to identify engineering
106 strategies that permit improved cell behavior in glutamine-free conditions. We thus screened
107 the CHO CRISPR knockout library cells for growth in media with and without glutamine for

108 fourteen days. The cells were passaged every three days (growth profile in Supplementary
109 Figure S1) and 30×10^6 cells were collected at the beginning and the end of the screen for
110 analysis to ensure adequate coverage.

111

112 **The gRNA library is well represented at the start of screening**

113 To ensure that all possible gene knockouts are screened it is important to verify that
114 the gRNA library is well represented at the beginning of the screen. We therefore sampled the
115 cells just prior to glutamine deprivation (T0) and sequenced the gRNAs present in the starting
116 cell pool. From the entire library, only 2 genes (<0.1%) and 638 gRNAs (<4%) were absent
117 at the initial time point. In all samples, median-normalized gRNA and gene sequencing depth
118 was greater than 35 and 360 CPM (counts per million), respectively (Figure 2). Thus, the
119 majority of the library was well represented before the CRISPR knockout library was subjected
120 to screening.

121

122 **Glutamine screening reveals expected and novel targets**

123 To identify gRNAs impacting CHO cell growth in glutamine free media, we analyzed
124 gRNA enrichment and depletion between samples grown for fourteen days in media with and
125 without glutamine. As expected, the absence of glutamine does not display a strong selection
126 pressure (Supplementary Figure S2), consistent with the ability of CHO cells to grow slowly
127 in the absence of glutamine due to low levels of endogenous glutamine synthetase
128 expression²⁹. We found 20 genes (Figure 3) that were significantly enriched or depleted in all
129 replicates. As expected, *Glnl* (glutamine synthetase) gRNAs showed significant depletion in

130 cells grown without glutamine, consistent with its role as the enzyme responsible for *de novo*
131 glutamine synthesis. Similarly, significant enrichment of *Gls* (glutaminase) gRNAs was
132 observed, consistent with protection of the intracellular glutamine pool from undesirable
133 catabolism when glutamine is not readily available.

134

135 **Disruption of *Abhd11* is conditionally beneficial dependent on presence of glutamine**

136 We found the strongest and most consistent gRNA enrichment in cells grown without
137 glutamine was a poorly characterized putative lipase, *Abhd11*. We subsequently generated
138 clonal *Abhd11* knockout cell lines using CRISPR-Cas9 and assessed their growth in media with
139 and without glutamine. In accordance with the screen, knocking out *Abhd11* substantially
140 improved growth in glutamine-free medium (Figure 4A) but also depressed growth in
141 glutamine containing medium compared to control cells (Figure 4B).

142

143 *Abhd11* has been poorly studied and is currently annotated as a putative lipase.
144 However, recent work reports that Abhd11 associates with the alpha-ketoglutarate
145 dehydrogenase complex (α kgdhc) and prevents its de-lipoylation³⁰ (a crucial cofactor for its
146 activity). The *Abhd11* knockout would thus be expected to decrease α kgdhc activity. The
147 benefit of the knockout in glutamine-free (and detriment in glutamine replete) conditions is
148 congruous with this mechanism. In the presence of glutamine, wildtype cells fuel the TCA
149 cycle heavily via glutaminolysis³¹, without Abhd11, α kgdhc activity would be attenuated and
150 entry of glutamine to the TCA cycle would be stunted. Consistent with this, we observe
151 drastically increased glutamate secretion in KO cells when grown in media containing

152 glutamine (Figure 5) and decreased glutamine uptake (KO cultures maintain >3 mM glutamine
153 at all timepoints while wildtype cells consume all glutamine by day 5 or 6, data not shown).

154

155 In the absence of glutamine, the decrease in α kgdhc activity in knockout cells would
156 act as an artificial bottleneck at alpha-ketoglutarate (α kg), forcing carbon away from the TCA
157 cycle and into glutamine biosynthesis. Thus, control cells, with functional *Abhd11*, would
158 consume α kg via α kgdhc to a greater extent than knockout cells, pulling away from *de novo*
159 glutamine synthesis, which is essential for growth in glutamine-free medium. Indeed, when
160 cells are adapted via stepwise decreases in glutamine levels and directed evolution³², cells adapt
161 by decreasing their expression of *Abhd11* (Supplementary Datafile 2). An overview of the
162 putative impact of *Abhd11* on glutamine metabolism is shown in Figure 6.

163 To explore the relationship between *Abhd11* and glutamine metabolism, we further
164 analyzed knockout and control cell lines and compared their transcriptomic profile when
165 grown in media with and without glutamine (Supplementary Methods and Results).

166

167 **Discussion**

168 As CHO cells are the primary workhorse for the production of biopharmaceuticals,
169 significant time and effort has been invested towards producing optimal cell lines for growth,
170 high protein titer, and good protein quality. Here, we present a high-throughput approach to
171 identify novel targets for CHO cell line engineering. The objective was two-fold: first to
172 establish a CHO-specific metabolic CRISPR-Cas9 knockout screening platform in CHO cells
173 and second to use this platform to explore CHO cell metabolism using an industrially relevant

174 screening setup. Glutamine is one of the major nutrients taken up by mammalian cells and
175 plays an important role as an energy source in *in vitro* culture^{25,33}. The fast consumption of
176 glutamine results in accumulated ammonia in the medium, inhibiting cell growth, reducing
177 productivity, and altering glycosylation patterns on heterologously expressed proteins^{5,27,34}.
178 While growth on glutamine-free media is possible, a significant decrease in growth rate is
179 almost always observed³⁵. It is therefore of interest to investigate genetic alterations that elicit
180 a positive growth response to media lacking glutamine. We found several genes whose
181 knockout resulted in a growth benefit in media without glutamine. Unsurprisingly, one of these
182 genes was *Gls*, which codes for the primary glutamine-catabolizing enzyme. Many of the
183 remaining targets found were novel with respect to their protective role in glutamine depletion
184 in CHO cells and their roles in a biological context are a topic for further investigation. We
185 chose to follow up on *Abhd11*, a gene with no clear link to glutamine metabolism that showed
186 the most marked enrichment of gRNAs in cells grown under glutamine depleted compared to
187 glutamine replete conditions. Our results are consistent with recent evidence linking *Abhd11*
188 with a protective role of α -kgdhc in the TCA cycle³⁶. We observed depressed growth of *Abhd11*
189 knockout cells in glutamine containing media alongside glutamate accumulation in the media
190 and lack of complete glutamine consumption. As glutamate (via glutaminolysis) is a major
191 source of TCA cycle intermediates³¹, the secretion of glutamate (and assumed decrease in TCA
192 cycle activity) is consistent with the observed reduced growth rate. Conversely, in glutamine
193 free media, *Abhd11* knockout cells exhibited improved growth compared to the wild type cells.
194 We postulate that the inhibition of α -ketoglutarate catabolism leads to accumulation of α -

195 ketoglutarate and increases its availability for conversion to glutamate and subsequently to
196 glutamine, leading to better growth.

197 High-throughput CRISPR-Cas9 screening presents a novel approach to conduct
198 forward genetic engineering and can provide an abundance of knowledge in the study of
199 genotype to phenotype relationships. Over recent years CRISPR-Cas9 screens have been
200 applied to a variety of mammalian cell types to study biological function^{20,21,37}. Since the
201 publication of initial CRISPR-Cas9 screens, comprehensive reviews and extensive method
202 articles have been published³⁸⁻⁴⁰. We show here that CRISPR screening techniques can be
203 applied to the industrially relevant CHO cell line. This approach enables a wide array of studies
204 in CHO cells by applying different screening conditions or exploiting the existing variations
205 of the Cas protein, such as catalytically inactive Cas9 coupled to transcriptional activators and
206 repressors, for activation or repression screens as has shown potential in other mammalian
207 cells^{39,41-45}. With continuous advances in CRISPR screen design and comprehensive
208 annotation of the CHO cell genome these types of screens will enable a new era of targeted
209 engineering to improve CHO cell phenotypes.

210

211 **Methods**

212 **Plasmid design and construction**

213 The GFP_2A_Cas9 plasmid was constructed as previously described⁴⁶. A Cas9
214 expression vector for generation of a Cas9 expressing CHO cell line (from here on be referred
215 to as CHO-SCas9), was constructed by cloning the 2A peptide-linked Cas9 ORF from the
216 GFP_2A_Cas9 expression vector⁴⁶ into a pcDNATM3.1(+) vector (Thermo Fisher Scientific)

217 between the HindIII and BamHI sites. The construct will from here on be referred to as
218 pcCas9. gRNA vectors were constructed using Uracil-Specific Excision Reagent (USER)
219 friendly cloning as previously described⁴⁷. Plasmids were purified using NucleoBond Xtra Midi
220 EF (Macherey-Nagel) according to manufacturer's protocol. Target sequences and gRNA
221 oligos are listed in Supplementary Table S2.

222

223 **Cell culture**

224 CHO-S wild type cells from Life Technologies were cultivated in CD-CHO medium
225 (Thermo Fisher Scientific) supplemented with 8 mM L-Glutamine and 2 µL/mL
226 AntiClumping Agent (AC) (Thermo Fisher Scientific) in a humidified incubator at 37 °C, 5 %
227 CO₂ at 120 RPM shake in sterile Corning® Erlenmeyer culture flasks (Sigma-Aldrich) unless
228 otherwise stated. Viable cell density (VCD) was measured using the NucleoCounter®
229 NC200™ (Chemometec) utilizing fluorescent dyes acridine orange and 4',6-diamidino-
230 2phenylindole (DAPI) for the detection of total and dead cells. Cells were seeded at 0.3 x 10⁶
231 cells/mL every three days or 0.5 x 10⁶ cells every two days.

232

233 **Transfection and cell line generation**

234 For all transfections, CHO-S wild type cells at a concentration of 1 x 10⁶ cells/mL in a
235 six well plate (BD Biosciences) in AC free media were transfected with a total of 3.75 µg DNA
236 using FreeStyleTM MAX reagent together with OptiPRO SFM medium (Life Technologies)
237 according to the manufacturer's instructions. For generation of CHO-SCas9, CHO-S wild type
238 cells were transfected with pcCas9. Stable cell pools were generated by seeding transfected

239 cells at 0.2 x 10⁶ cells/mL in 3 mL selection media containing 500 µg/mL G418
240 (SigmaAldrich) in CELLSTAR® 6 well Advanced TC plates (Greiner Bio-one) two days post
241 transfection. Medium was changed every four days during selection. After two weeks of
242 selection, cells were detached and adapted to grow in suspension. The clonal cell lines were
243 analysed by Celigo Cell Imaging Cytometer (Nexcelom Bioscience) based on the green
244 fluorescence level using the mask (blue fluorescence representing individual cells stained with
245 NucBlue™ Live ReadyProbes™ Reagent; Thermo Fisher Scientific) + target 1 (green
246 fluorescence) application. For generating knockout cell lines of screen targets, CHO-S wild
247 type cells were transfected with GFP_2A_Cas9 and appropriate gRNA expression vectors at
248 a DNA ratio of 1:1 (w:w). Two days after transfection cells were single cell sorted using a
249 FACSJazz (BD Bioscience), gating for GFP positive cell population as described previously⁴⁶.
250 Indels in targeted genes were verified by Next Generation Sequencing (NGS) as described
251 previously⁴⁶. Primers are listed in Supplementary Table S2. Three clones with a confirmed
252 indel and two control clones without indels were expanded to 30 mL media before they
253 were frozen down at 1 x 10⁷ cells per vial in spent CD-CHO medium with 5 % DMSO (Sigma-
254 Aldrich).

255

256 **Characterizing CHO-S^{Cas9} functionality**

257 To characterize Cas9 functionality we transfected clonal CHO-S^{Cas9} cells with a vector
258 expressing gRNA against Mgat1 and verified indel generation on a pool level by NGS as
259 described previously⁴⁸ (using gRNA oligo primers MGAT1_gRNA_fwd and
260 MGAT1_gRNA_rev and NGS primers MGAT1_miseq_fwd and MGAT1_miseq_rev listed

261 in Supplementary Table S2). To analyze GFP expression, clonal cells were seeded in wells of
262 a 96-well optical-bottom microplate (Greiner Bio-One) and identified GFP positive cells on
263 the Celigo Cell Imaging Cytometer (Nexcelom Bioscience) using the green fluorescence
264 channel. GFP negative gating was set on the basis of fluorescence emitted from CHO-S wild
265 type cells.

266

267 **Library design and construction**

268 For design of the metabolic gRNA library, a list of metabolic genes was extracted from
269 the CHO metabolic network reconstruction³ along with a list of genes with metabolic GO
270 terms in CHO and associated transcription factors. The gRNA templates were
271 computationally designed using CRISPy (<http://crispy.biosustain.dtu.dk/>), resulting in a
272 gRNA library with a minimum of 5 gRNAs per gene. The oligo library was synthesized by
273 CustomArray. Full-length oligonucleotides were amplified by PCR using KAPA Hifi (Kapa
274 Biosystems), size selected on a 2% agarose gel and purified with a QIAquick Gel Extraction
275 Kit (Qiagen) as per manufacturer's protocol. The gRNA-LGP vector (Addgene #52963) was
276 digested using BsmBI (New England BioLabs) (4 µg gRNA-LGP vector, 5 µL buffer 3.1, 5
277 µL 10 x BSA, 3 µL BsmBI and H2O up to 50 µL were mixed and incubated at 55°C for 3
278 hours). Subsequently, 2 µL of calf intestinal alkaline phosphatase (New England BioLabs) was
279 added to the digested vector and the mix was incubated at 37°C for 30 minutes before it was
280 purified with a QIAquick PCR Purification Kit (Qiagen) as per manufacturer's protocol. To
281 assemble the gRNAs into the vector a 20 µL Gibson ligation reaction (New England BioLabs)
282 was carried out (25 ng linearized vector, 10 ng purified insert, 10 µL 2 x Gibson Assembly

283 Master Mix (New England BioLabs) and up to 20 μ L H₂O were mixed and incubated at 50°C
284 for 1 hour). The assembled vector was purified using QIAquick PCR purification (Qiagen)
285 and transformed into chemically competent E. coli (Invitrogen). Transformed bacteria were
286 plated onto LB-carbenicillin plates for overnight incubation at 37°C, and plasmid DNA was
287 purified using a HiSpeed Plasmid Maxi Kit (Qiagen).

288

289 **Lentiviral packaging**

290 To produce the lentivirus, HEK293T cells were cultivated in DMEM supplemented
291 with 10% Fetal Bovine Serum (FBS). One day prior to transfection, cells were seeded in a
292 15cm tissue culture plate at a density suitable for reaching 70-80% confluency at time of
293 transfection. Culture medium was replaced with prewarmed DMEM containing 10% FBS. 36
294 μ L Lipofectamine 3000 (Life Technologies) was diluted in 1.2 mL OptiMEM
295 (LifeTechnologies) and in a separate tube 48 μ L P3000 reagent, 12 μ g pCMV (Addgene
296 #12263), 3 μ g pMD2.G (Addgene #12259) and 9 μ g lentiviral vector were diluted in 1.2 mL
297 OptiMEM. The solutions were incubated for 5 minutes at room temperature, mixed,
298 incubated for another 30 minutes before they were added dropwise to the HEK293T cells. 48
299 hours and 72 hours after transfection the viral particles were concentrated using Centricon
300 Plus-20 Centrifugal ultrafilters (100 kDa pore size), aliquoted and stored at -80°C.

301

302 **Puromycin kill curve**

303 To determine the concentration of puromycin to be used to select the CHO library
304 cells for gRNA insertion, a puromycin kill curve for CHO cells was determined. CHO-S wild

305 type cells at a concentration of 1×10^6 cells/mL in media containing various amounts of
306 puromycin (0, 0.25, 0.5, 1, 2, 3, 4, 5, 6, 7, 8 and 10 $\mu\text{g}/\text{mL}$). Cell viability and VCD was
307 monitored over 7 days and based on halted growth and complete cell death of wild type cells
308 10 $\mu\text{g}/\text{mL}$ was used for further experiments (Supplementary Figure S3).

309

310 **Transducing CHO-S^{Cas9} with library virus**

311 CHO-S^{Cas9} cells were seeded at 0.3×10^6 cells/mL in 1 mL media in 26 wells of 12 well
312 plates (BD Biosciences). In 25 of the wells, cells were transduced with 4 μL library virus/well
313 along with 8 $\mu\text{g}/\text{mL}$ Polybrene (Sigma-Aldrich) aiming for an MOI at 0.3-0.4 (Supplementary
314 Methods and Results). Cells in the remaining well were left non-transduced as a negative
315 control. After 24 hours, the cells were washed in PBS (Sigma-Aldrich) by centrifugation at 200
316 $\times g$, resuspended in media and seeded in a new 12 well plate. After 24 hours, cells were
317 expanded to 3 mL media in wells of 6 well plates (BD Biosciences). Selection for cells
318 containing the gRNA insert was initiated by adding 10 $\mu\text{g}/\text{mL}$ puromycin (Thermo Fisher
319 Scientific) to each well (see puromycin kill curve in Supplementary Figure S3). Non-transduced
320 control cells were monitored for complete cell death, equating finalised selection. The cells
321 were washed and passed twice before they were expanded to attain enough cells to create a
322 cell bank. Cells were frozen down at 1×10^7 cells per vial in spent CD-CHO medium with 5
323 % DMSO (SigmaAldrich) and will from here on be referred to as CHO-S^{Cas9} library cells.

324

325

326

327 **Screening and DNA extraction**

328 CHO-S^{Cas9} library cells were thawed in 30 mL media and expanded to 60 mL before
329 starting the screen. On day 0 (T0) 1.5 x 10⁷ cells were spun down at 200 x g and resuspended
330 in 60 mL appropriate screening media. The cells were grown for 14 days (passed to 0.25 x 10⁶
331 cells/mL every third day). 30 x 10⁶ cells were collected at T0 and on day 14 (T14). The pellets
332 were stored at -80°C until further use. gDNA extraction of all 30 x 10⁶ cells was carried out
333 using GeneJET Genomic DNA Purification Kit (Thermo Fisher Scientific) following the
334 manufacturer's protocol. gDNA was eluted in 100 µL preheated elution buffer from the
335 purification kit and incubated for 10 minutes before final centrifugation for maximum gDNA
336 recovery.

337

338 **Preparation for next generation sequencing**

339 50 µL PCR reactions with 3 µg input gDNA per reaction were run using Phusion®
340 Hot Start II High-Fidelity DNA Polymerase (Thermo Fisher Scientific) (95°C for 4 min; 30
341 times: 98°C for 45s, 60°C for 30 s, 72°C for 1 min; 72°C for 7 min) using primers flanking the
342 gRNA insert containing overhang sequenced compatible with Illumina Nextera XT indexing
343 and 8 random nucleotides to increase the diversity of the sequences (LIB_8xN_NGS_FWD
344 and LIB_8xN_NGS_REV listed in Supplemental Table S2). Double size selection was
345 performed using Agencourt AMPure XP beads (Beckman Coulter) to exclude primer dimers
346 and genomic DNA. The amplicons were indexed using Nextera XT Index Kit v2 (Illumina)
347 sequence adapters using KAPA HiFi HotStart ReadyMix (KAPA Biosystems) (95°C for 3 min;
348 8 times: 95°C for 30s, 55°C for 30 s, 72°C for 30 s; 72°C for 5 min) and subjected to a second

349 round of bead-based size exclusion. The resulting library was quantified with Qubit® using
350 the dsDNA HS Assay Kit (Thermo Fisher Scientific) and the fragment size was determined
351 using a 2100 Bioanalyzer Instrument (Agilent) before running the samples on a NextSeq 500
352 sequencer (Illumina).

353

354 **Analysis**

355 Raw FASTQ files for samples from the end time points of glutamine selection were
356 uploaded to PinAPL-PY (<http://pinapl-py.ucsd.edu/>)⁴⁹ along with a file containing the
357 sequences for all gRNAs contained in the library. Top candidates for enriched and for depleted
358 gRNAs were ranked by an adjusted robust rank aggregation (aRRA) method⁵⁰ and filtered for
359 significance, compared between the replicates and used for verification of the screen. The
360 screen was analyzed using default parameters set by PinAPL-PY.

361

362 **Batch culture**

363 *Abhd11* knockout cell lines were seeded at 0.3×10^6 cells/mL in 90 mL CD-CHO media
364 with and without glutamine supplemented with 1 μ L/mL AC in 250 mL Corning® Erlenmeyer
365 culture flasks (Sigma-Aldrich). Cell viability and density were measured every day for a
366 maximum of fourteen days.

367

368 **Analysis of cell line adapted to absence of glutamine by directed evolution**

369 A previously established cell line that was adapted to grow without glutamine by
370 stepwise decrease in glutamine concentration and directed evolution³² was grown in batch

371 culture as previously described⁵¹. Samples were taken at the same time points and analysed
372 using a mouse Agilent 22 k microarray (G4121B) platform as described for the parental cell
373 line grown in medium with 8mM glutamine⁵¹. Differential transcriptome and statistical
374 analyses were performed as previously described⁵¹.

375

376 **Acknowledgements**

377 The authors wish to thank Nachon Charanyanonda Petersen for assistance, cell line
378 generation and batch culture and Anna Koza, Alexandra Hoffmeyer, Pannipa Pornpitapong
379 for assistance with NGS, Dr. Prashant Mali for packaging the gRNA library into the lentivirus,
380 Dr. James A Nathan for discussions regarding *Abhd11* and Daria Sergeeva for co-drawing
381 Figure 1. This work was supported by the Novo Nordisk Foundation (NNF10CC1016517
382 and NNF16OC0021638) and NIGMS (R35 GM119850, NEL).

383

384

385

386

387

388

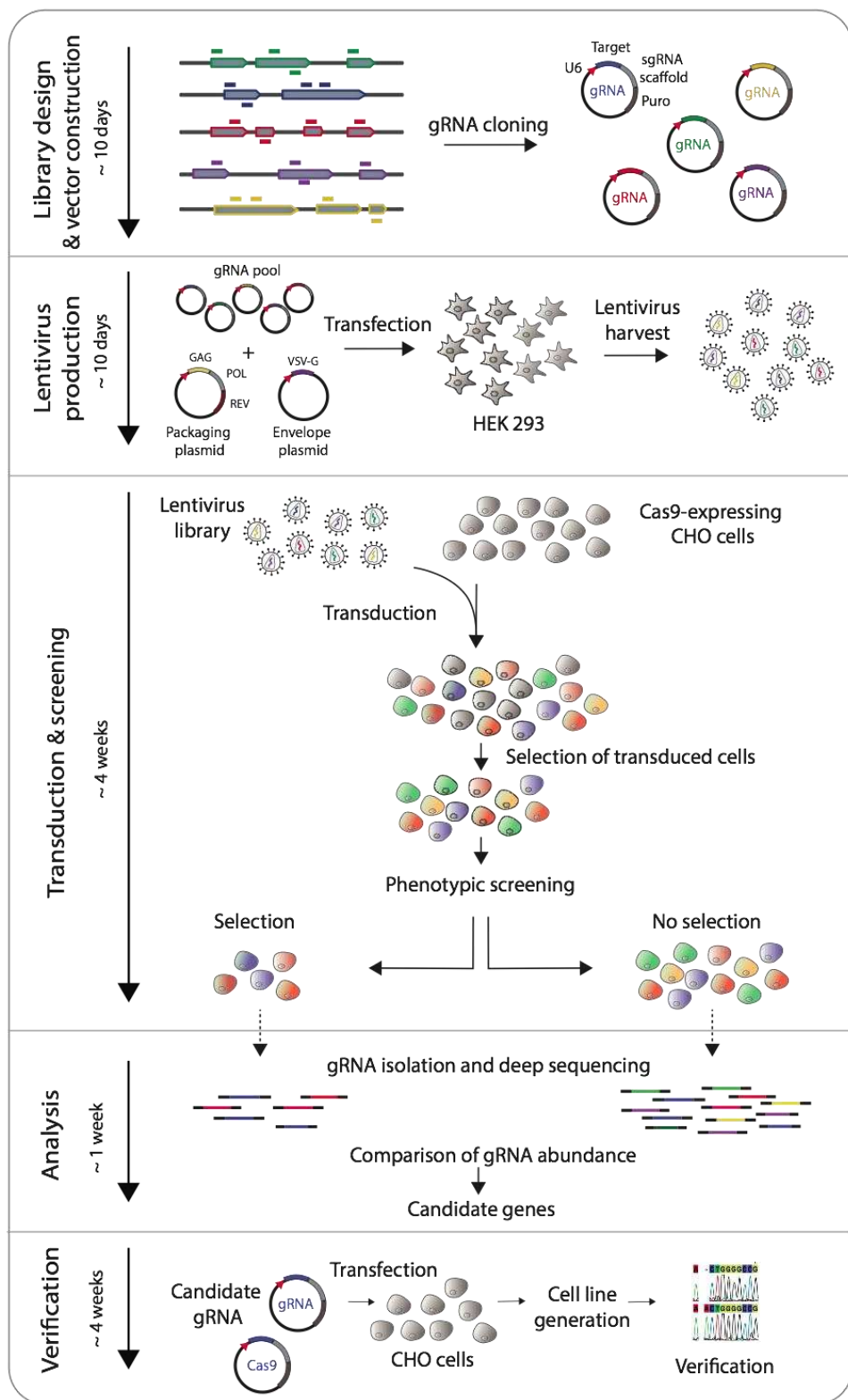
389

390

391

392

393 **Figures**

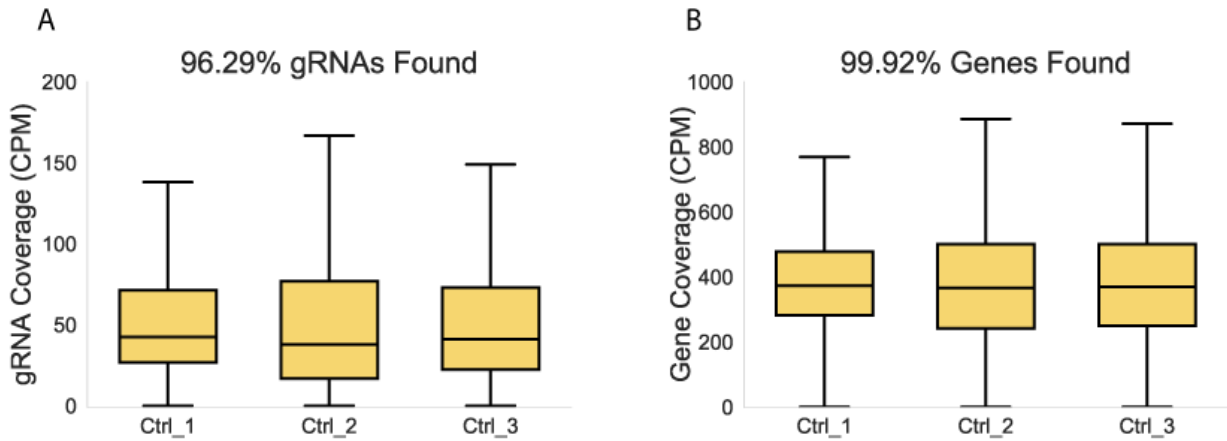


395 **Figure 1 Screening overview**

396 gRNAs are computationally designed to target the genes of interest, then synthesized and cloned into gRNA
397 scaffold containing vectors. HEK cells are transfected with packaging vectors and gRNA vectors to generate a
398 pool of viruses containing all the gRNA vectors. After harvest, the pooled library is used to transduce Cas9-
399 expressing CHO cells at a low MOI to ensure a single integration event per cell. Cells positive for gRNA
400 integration are selected for with antibiotics before undergoing a phenotypic screen. Genomic DNA is extracted
401 from the collected cells and gRNA presence is compared between samples. Enriched or depleted gRNAs are
402 ranked and candidate genes are phenotypically validated.

403

404



405

406 **Figure 2 Screen verification**

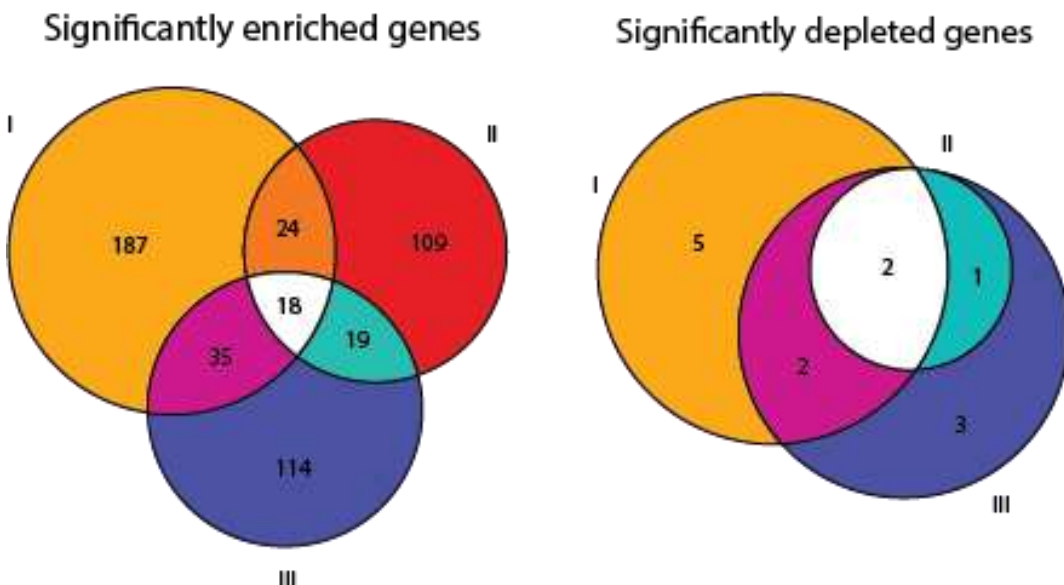
407 A) Read count per gRNA. B) Total read count per gene (summed over all gRNAs). Shown are normalized read
408 counts (counts per million/CPM) for three replicate experiments prior to starting selection. Outliers not
409 displayed.

410

411

412

413



414

415

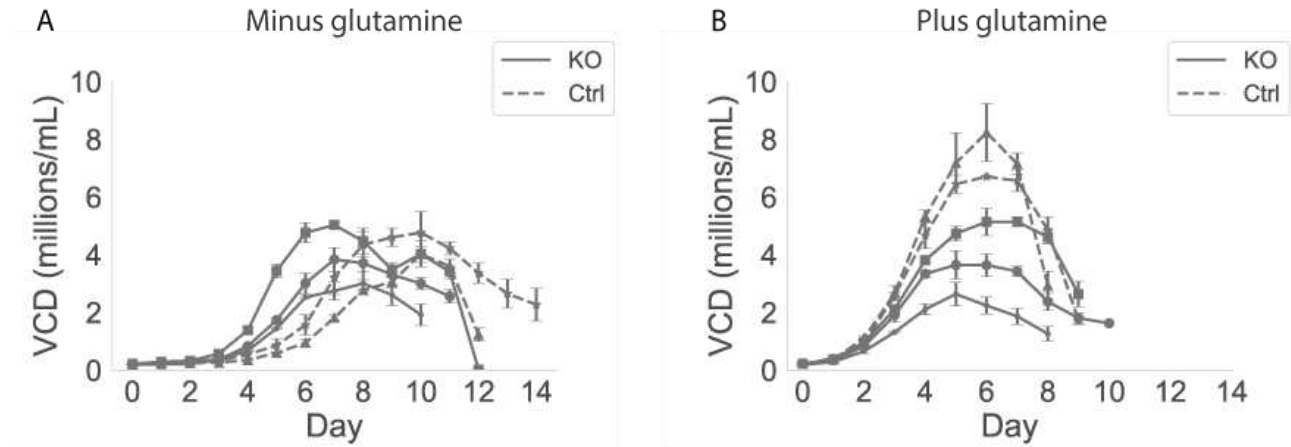
416 **Figure 3 Significantly enriched and depleted genes following glutamine selection**

417 Three glutamine screens of the knockout library were carried out and the significantly depleted and enriched
418 genes from each replicate are shown. While there was variability between replicates (I-III), eighteen significantly
419 enriched genes and two significantly depleted genes were commonly observed in all experiments.

420

421

422



423

424 **Figure 4 Growth curves for *Abhd11* knockout and control cell lines in batch culture in media without**
425 **and with glutamine**

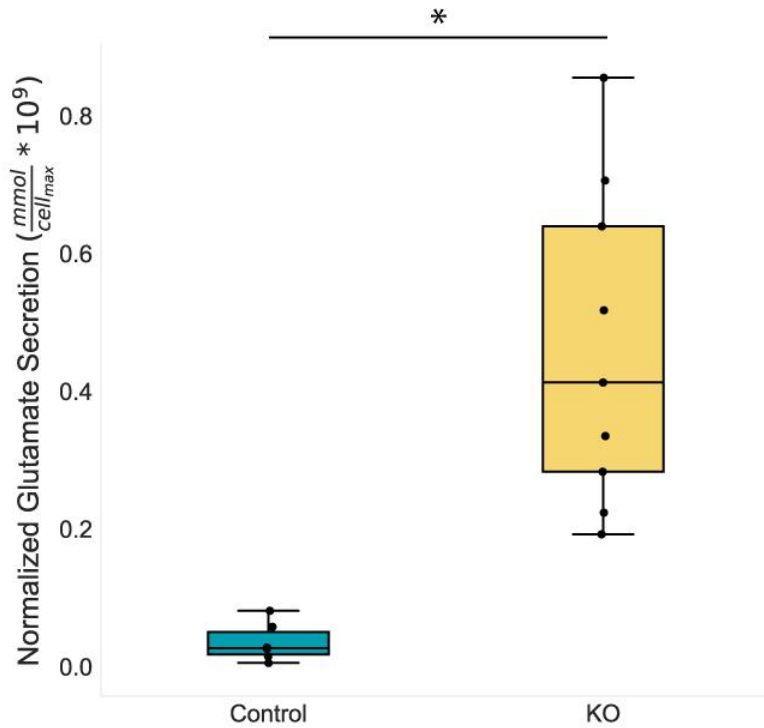
426 Growth curves for three *Abhd11* knockout (KO) and two control (Ctrl) cell lines grown in three replicates in
427 media without glutamine (A) and with glutamine (B). Viable cell density (VCD) was measured every day over a
428 period of 14 days.

429

430

431

432



433

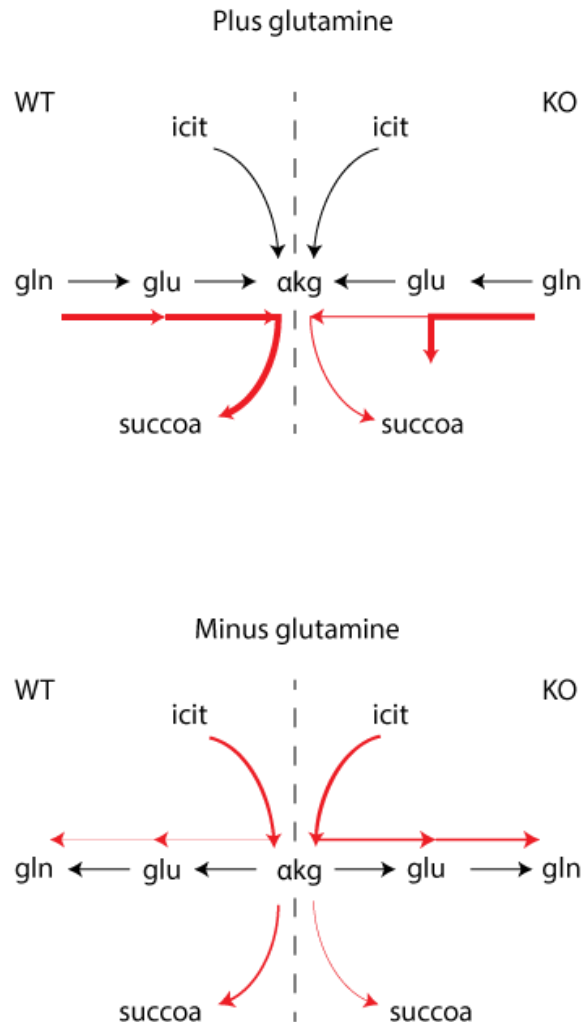
434 **Figure 5 Impact of *Abhd11* knockout on glutamate secretion**

435 Wild type (control) and knockout cells were grown in glutamine replete conditions. Glutamate secreted during
436 the growth phase (e.g., until maximum VCD was reached) was normalized by the maximum VCD to
437 approximate cell specific glutamate secretion. Knockout cells secreted significantly more glutamate than
438 wildtype cells. * indicates a statistically significant difference ($p < 0.05$) as calculated by a two-tailed Welch's t-
439 test.

440

441

442



443

444

445 **Figure 6 Putative mechanism of action for wild type (WT) and *Abhd11* knockout (KO) cells grown in**
446 **media with or without glutamine.**

447 *Abhd11* associates with and protects the α kgdhc. (a) In the presence of gln, cells fuel the TCA cycle through
448 gln catabolism. In *Abhd11* KO cell lines, α kgdhc flux (and TCA cycle activity) is decreased, α kg and glu
449 accumulate, and glu is secreted, leading to decreased growth for KO cells. (b) Without gln, the TCA cycle is
450 largely fueled through glycolysis. In *Abhd11* KO cell lines, the decrease in α kgdhc activity leads to increased
451 α kg, which permits increased flux to glu and *de novo* glutamine synthesis. With normal *Abhd11* function, cells
452 do not have this bottleneck and α kgdhc activity competes more strongly with gln biosynthesis, leading to
453 decreased growth for WT cells. α kgdhc: alpha ketoglutarate complex, icit: isocitrate, α kg: alpha-ketoglutarate,
454 succoa: succinyl coenzyme A, gln: glutamine, glu: glutamate.

455

456 References

457 1. Walsh, G. Biopharmaceutical benchmarks 2018. *Nat. Biotechnol.* **36**, 1136–1145 (2018).

458 2. Jayapal, K. P., Wlaschin, K. F., Hu, W. S. & Yap, M. G. S. Recombinant Protein Therapeutics from
459 CHO Cells — 20 Years and Counting. *Chemical Engineering Progress* vol. 103 40–47 (2007).

460 3. Hefzi, H. *et al.* A Consensus Genome-scale Reconstruction of Chinese Hamster Ovary Cell
461 Metabolism. *Cell Syst* **3**, 434–443.e8 (2016).

462 4. Zielinski, D. C. *et al.* Systems biology analysis of drivers underlying hallmarks of cancer cell metabolism.
463 *Sci. Rep.* **7**, 41241 (2017).

464 5. Yang, M. & Butler, M. Effects of ammonia on CHO cell growth, erythropoietin production, and
465 glycosylation. *Biotechnol. Bioeng.* **68**, 370–380 (2000).

466 6. Hansen, H. A. & Emborg, C. Influence of ammonium on growth, metabolism, and productivity of a
467 continuous suspension Chinese hamster ovary cell culture. *Biotechnol. Prog.* **10**, 121–124 (1994).

468 7. Hassell, T., Gleave, S. & Butler, M. Growth inhibition in animal cell culture. The effect of lactate and
469 ammonia. *Appl. Biochem. Biotechnol.* **30**, 29–41 (1991).

470 8. Ozturk, S. S., Riley, M. R. & Palsson, B. O. Effects of ammonia and lactate on hybridoma growth,
471 metabolism, and antibody production. *Biotechnol. Bioeng.* **39**, 418–431 (1992).

472 9. Brinkrolf, K. *et al.* Chinese hamster genome sequenced from sorted chromosomes. *Nat. Biotechnol.* **31**,
473 694–695 (2013).

474 10. Lewis, N. E. *et al.* Genomic landscapes of Chinese hamster ovary cell lines as revealed by the *Cricetulus*
475 *griseus* draft genome. *Nat. Biotechnol.* **31**, 759–765 (2013).

476 11. Xu, X. *et al.* The genomic sequence of the Chinese hamster ovary (CHO)-K1 cell line. *Nat. Biotechnol.*
477 **29**, 735–741 (2011).

478 12. Gutierrez, J. M. & Lewis, N. E. Optimizing eukaryotic cell hosts for protein production through
479 systems biotechnology and genome-scale modeling. *Biotechnol. J.* **10**, 939–949 (2015).

480 13. Santiago, Y. *et al.* Targeted gene knockout in mammalian cells by using engineered zinc-finger

481 nucleases. *Proc. Natl. Acad. Sci. U. S. A.* **105**, 5809–5814 (2008).

482 14. Sakuma, T. *et al.* Homologous Recombination-Independent Large Gene Cassette Knock-in in CHO
483 Cells Using TALEN and MMEJ-Directed Donor Plasmids. *Int. J. Mol. Sci.* **16**, 23849–23866 (2015).

484 15. Cullen, L. M. & Arndt, G. M. Genome-wide screening for gene function using RNAi in mammalian
485 cells. *Immunol. Cell Biol.* **83**, 217–223 (2005).

486 16. Klanert, G. *et al.* A cross-species whole genome siRNA screen in suspension-cultured Chinese hamster
487 ovary cells identifies novel engineering targets. *Sci. Rep.* **9**, 8689 (2019).

488 17. Smith, I. *et al.* Evaluation of RNAi and CRISPR technologies by large-scale gene expression profiling in
489 the Connectivity Map. *PLoS Biol.* **15**, e2003213 (2017).

490 18. Kaelin, W. G., Jr. Molecular biology. Use and abuse of RNAi to study mammalian gene function. *Science*
491 **337**, 421–422 (2012).

492 19. Hart, T., Brown, K. R., Sircoulomb, F., Rottapel, R. & Moffat, J. Measuring error rates in genomic
493 perturbation screens: gold standards for human functional genomics. *Mol. Syst. Biol.* **10**, 733 (2014).

494 20. Koike-Yusa, H., Li, Y., Tan, E.-P., Velasco-Herrera, M. D. C. & Yusa, K. Genome-wide recessive
495 genetic screening in mammalian cells with a lentiviral CRISPR-guide RNA library. *Nat. Biotechnol.* **32**,
496 267–273 (2014).

497 21. Shalem, O. *et al.* Genome-scale CRISPR-Cas9 knockout screening in human cells. *Science* **343**, 84–87
498 (2014).

499 22. Zhou, Y. *et al.* High-throughput screening of a CRISPR/Cas9 library for functional genomics in human
500 cells. *Nature* **509**, 487–491 (2014).

501 23. Bassett, A. R., Kong, L. & Liu, J.-L. A genome-wide CRISPR library for high-throughput genetic
502 screening in Drosophila cells. *J. Genet. Genomics* **42**, 301–309 (2015).

503 24. Krämer, A., Green, J., Pollard, J., Jr & Tugendreich, S. Causal analysis approaches in Ingenuity Pathway
504 Analysis. *Bioinformatics* **30**, 523–530 (2014).

505 25. Yao, T. & Asayama, Y. Animal-cell culture media: History, characteristics, and current issues. *Reprod.*
506 *Med. Biol.* **16**, 99–117 (2017).

507 26. Borys, M. C., Linzer, D. I. & Papoutsakis, E. T. Ammonia affects the glycosylation patterns of
508 recombinant mouse placental lactogen-I by chinese hamster ovary cells in a pH-dependent manner.
509 *Biotechnol. Bioeng.* **43**, 505–514 (1994).

510 27. Thorens, B. & Vassalli, P. Chloroquine and ammonium chloride prevent terminal glycosylation of
511 immunoglobulins in plasma cells without affecting secretion. *Nature* **321**, 618–620 (1986).

512 28. Taschwer, M. *et al.* Growth, productivity and protein glycosylation in a CHO EpoFc producer cell line
513 adapted to glutamine-free growth. *Journal of Biotechnology* vol. 157 295–303 (2012).

514 29. Fan, L. *et al.* Improving the efficiency of CHO cell line generation using glutamine synthetase gene
515 knockout cells. *Biotechnol. Bioeng.* **109**, 1007–1015 (2012).

516 30. Bailey, P. S. J. *et al.* ABHD11 regulates 2-oxoglutarate abundance by protecting mitochondrial lipoylated
517 proteins from lipid peroxidation damage. *bioRxiv* doi:10.1101/2020.04.18.048082.

518 31. Ahn, W. S. & Antoniewicz, M. R. Parallel labeling experiments with [1,2-(13)C]glucose and [U-
519 (13)C]glutamine provide new insights into CHO cell metabolism. *Metab. Eng.* **15**, 34–47 (2013).

520 32. Bort, J. A. H., Hernández Bort, J. A., Stern, B. & Borth, N. CHO-K1 host cells adapted to growth in
521 glutamine-free medium by FACS-assisted evolution. *Biotechnology Journal* vol. 5 1090–1097 (2010).

522 33. Newsholme, P. *et al.* Glutamine and glutamate as vital metabolites. *Braz. J. Med. Biol. Res.* **36**, 153–163
523 (2003).

524 34. Yang, M. & Butler, M. Effect of ammonia on the glycosylation of human recombinant erythropoietin in
525 culture. *Biotechnol. Prog.* **16**, 751–759 (2000).

526 35. Altamirano, C., Paredes, C., Cairo, J. J. & Godia, F. Improvement of CHO Cell Culture Medium
527 Formulation: Simultaneous Substitution of Glucose and Glutamine. *Biotechnol. Prog.* **16**, 69–75 (2000).

528 36. Bailey, P. S. J., Ortmann, B. M., Costa, A. S., Frezza, C. & Nathan, J. A. T6 Identification of ROLIP as
529 a mitochondrial regulator of metabolism and the hypoxia response pathway. *BTS/ BALR/ BLF Early*
530 *Career Investigator Awards Symposium* (2019) doi:10.1136/thorax-2019-btsabstracts2019.6.

531 37. Wang, T., Wei, J. J., Sabatini, D. M. & Lander, E. S. Genetic Screens in Human Cells Using the
532 CRISPR-Cas9 System. *Science* **343**, 80–84 (2014).

533 38. Schuster, A. *et al.* RNAi/CRISPR Screens: from a Pool to a Valid Hit. *Trends Biotechnol.* **37**, 38–55
534 (2019).

535 39. Joung, J. *et al.* Genome-scale CRISPR-Cas9 knockout and transcriptional activation screening. *Nat.*
536 *Protoc.* **12**, 828–863 (2017).

537 40. Doench, J. G. Am I ready for CRISPR? A user's guide to genetic screens. *Nat. Rev. Genet.* **19**, 67–80
538 (2017).

539 41. Gilbert, L. A. *et al.* Genome-Scale CRISPR-Mediated Control of Gene Repression and Activation. *Cell*
540 **159**, 647–661 (2014).

541 42. Joung, J. *et al.* Genome-scale activation screen identifies a lncRNA locus regulating a gene
542 neighbourhood. *Nature* **548**, 343–346 (2017).

543 43. Heaton, B. E. *et al.* A CRISPR Activation Screen Identifies a Pan-avian Influenza Virus Inhibitory Host
544 Factor. *Cell Rep.* **20**, 1503–1512 (2017).

545 44. Liu, S. J. *et al.* CRISPRi-based genome-scale identification of functional long noncoding RNA loci in
546 human cells. *Science* **355**, (2017).

547 45. Rosenbluh, J. *et al.* Complementary information derived from CRISPR Cas9 mediated gene deletion
548 and suppression. *Nat. Commun.* **8**, 15403 (2017).

549 46. Grav, L. M. *et al.* One-step generation of triple knockout CHO cell lines using CRISPR/Cas9 and
550 fluorescent enrichment. *Biotechnol. J.* **10**, 1446–1456 (2015).

551 47. Ronda, C. *et al.* Accelerating genome editing in CHO cells using CRISPR Cas9 and CRISPy, a web-
552 based target finding tool. *Biotechnol. Bioeng.* **111**, 1604–1616 (2014).

553 48. Lee, J. S., Kallehauge, T. B., Pedersen, L. E. & Kildegaard, H. F. Site-specific integration in CHO cells
554 mediated by CRISPR/Cas9 and homology-directed DNA repair pathway. *Sci. Rep.* **5**, 8572 (2015).

555 49. Spahn, P. N. *et al.* PinAPL-Py: A comprehensive web-application for the analysis of CRISPR/Cas9
556 screens. *Sci. Rep.* **7**, 15854 (2017).

557 50. Li, W. *et al.* MAGECK enables robust identification of essential genes from genome-scale
558 CRISPR/Cas9 knockout screens. *Genome Biol.* **15**, 554 (2014).

559 51. Hernández Bort, J. A. *et al.* Dynamic mRNA and miRNA profiling of CHO-K1 suspension cell
560 cultures. *Biotechnol. J.* **7**, 500–515 (2012).